

# LANDSLIDE SUSCEPTIBILITY MAPPING USING FREQUENCY RATIO-BASED FUZZY LOGIC APPROACH IN LIMA PULUH KOTA REGENCY

Surtani<sup>1</sup>, \*Ahyuni<sup>1</sup>, Hamdi Nur<sup>2</sup>, Alifah Tahsya<sup>1</sup>, Dina Rahayu Eliza Prisma<sup>1</sup>

<sup>1</sup>Department of Geography – Universitas Negeri Padang, Indonesia

<sup>2</sup> Department of Urban and Regional Planning, Universitas Bung Hatta, Indonesia

Email: ahyuniaziz@fis.unp.ac.id

\*Corresponding Author, Received: Aug 25, 2024. Revised: Nov 24, 2024. Accepted: Dec 05, 2024



This is an open access article distributed under the Creative Commons 4.0 Share-Alike 4.0 International License. If you remix, transform, or build upon the material, you must distribute your contributions under the same license as the original. ©2022 by Journal Sjdgge

**ABSTRACT:** One of the non-linear models for determining landslide-prone areas is the fuzzy logic method. This research aims to determine the landslide prone zoning map in Limapuluh Kota Regency, by using fuzzy gamma operations in GIS, from 11 factors: aspect, curvature, elevation, slope, landform, geology, proximity to stream, landcover, rainfall intensity, NDVI and soil. The data used is 149 landslide events in Limapuluh Kota Regency. The data was processed using the factors that cause landslides with a train and test ratio of 60: 40. The research results show that by using  $\gamma = 0.975$ , an area with high landslide characteristics was obtained covering an area of 28,463 ha (8.79%), with a medium area of 76,544 ha (23.64%) and low area of 218,820 (65.57%). By validating using the ROC curve and test data, an AUC value of 0.746 was obtained, which means the accuracy level of the resulting map is high

*Keywords: Landslide, fuzzy gamma, susceptibility map*

## 1. INTRODUCTION

Limapuluh Kota Regency is an area prone to landslides in West Sumatera. This regency connects West Sumatera Province and Riau Province. It was recorded that in 2017, there were 10 cases of landslides, 22 cases in 2018, 11 cases in 2019, 3 cases in 2020, 2 cases in 2021, 8 cases in 2022 and at the end of 2023 there were landslides on the West Sumatera-Riau route [1] (BPBD, 2023). For this reason, it is necessary to estimate the locations prone to landslides in Limapuluh Kota Regency.

Various methods are used to determine landslide susceptibility maps. Starting from heuristic, statistical and deterministic approaches [1](Ahyuni, Susetyo, B.B, Oktari, F., Nur, H., Aziz, 2021). Other researchers put forward 2 techniques, namely direct hazard mapping and indirect hazard mapping [2](Tangestani, 2009). It is directly related to the geomorphologist's determination of his knowledge of slope conditions, while indirectly it uses statistical models which are determined based on the factors that cause landslides and landslides events.

The use of statistical methods has been widely used as stated by [3](Mandal, S., Mondal, 2019). The use of statistical models is related to the data used in an area. Preparation of the data to be used (training data and its quality depends on the nature of the field investigation used. However, the model used will determine the data requirements [4] The

model used can be in linear or non-linear form [5] [6] [7] Examples of comparisons of statistical methods have been carried out by many experts, such as [8] [9] [10] [11].

The use of non-linear models between influencing factors and landslide events can be done with fuzzy membership functions with the help of GIS and raster domains. This has been done by several experts such as [12] [13] [14] [13] [15] [16]. In this study, fuzzy logic was applied to determine the landslide susceptibility zoning map in Limapuluh Kota Regency, Indonesia by determining factors in the occurrence of landslides with values between 0 and 1. Fuzzy gamma was used to determine the landslide susceptibility map.

## 2. METHODS

Preparation for making disaster prone maps was carried out using Gamma operations on fuzzy membership with the help of GIS. The data used includes aspect, curvature, elevation, slope, landform, geology, proximity to stream, landcover, rainfall intensity, NDVI and soil.

One of the methods used in the fuzzy gamma operator is Frequency Ratio. The ratio frequency of a particular class in a causal parameter can be obtained when compared with a landslide inventory.

**Frequency Ratio**

$$FR = \frac{N \text{ cell } (Li) / N \text{ cell } (ci)}{N \text{ cell } (L) / N \text{ cell } (C)}$$

*Information:*

N cell (Li) = the number of avalanche cells in a particular category

N cell (Ci) = the total number of avalanche cells in a particular category

N cell (L) = total number of avalanche cells

N cell (C) = number of cells

**Membership (FR)**

$$FR = \frac{X_{FR} - Min_{FR}}{Max_{FR} - Min_{FR}}$$

*Information:*

X<sub>FR</sub> = Frequency ratio value

Min<sub>FR</sub> = Minimum value of Frequency ratio

Max<sub>FR</sub> = Maximum value of Frequency ratio

**Operator Fuzzy**

**2.1. Fuzzy Algebraic Product**

$$\mu_{combination} = \prod_{i=1}^n \mu_i \dots \dots \dots (1)$$

Where,

μ<sub>i</sub> = Fuzzy membership function for map i (i = 1,2,...n maps to be combined

**2.2. Fuzzy Algebraic Sum**

$$\mu_{combination} = 1 - \prod_{i=1}^n (1 - \mu_i) \dots \dots \dots (2)$$

Where,

μ<sub>i</sub> = Fuzzy membership function for map i (i = 1,2,...n maps to be combined

**2.3. Fuzzy Gamma Operator**

The fuzzy gamma operator is a fuzzy operator for combining membership functions. The fuzzy gamma operator formula, ie:

$$Combination = (Fuzzy \ algebraic \ Sum)^\gamma \cdot (Fuzzy \ Algebraic \ Product)^{1-\gamma} \dots \dots \dots (3)$$

Where,

The exponent γ, which is a number from <0, 1> interval, allows optimization of the membership combination. Setting it to the extremes of the interval give either fuzzy algebraic sum (γ = 1) or fuzzy algebraic product (γ = 0)

Analysis of landslide hazard levels using Fuzzy overlay. The tools provided by GIS for fuzzy overlay consist of 5 operators, And, Or, Sum, Product and Gamma. In this study, the Gamma tools were used. In Fuzzy Gamma it is the result of Fuzzy Sum multiplied by Fuzzy Product. The study area and landslide events can be seen in figures 2 and 3.

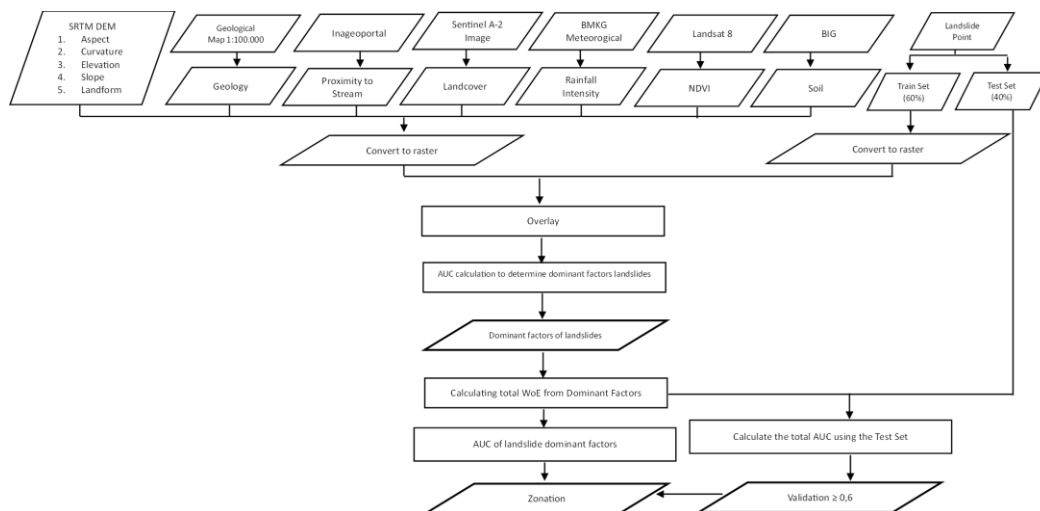


Fig. 1 Research Flow

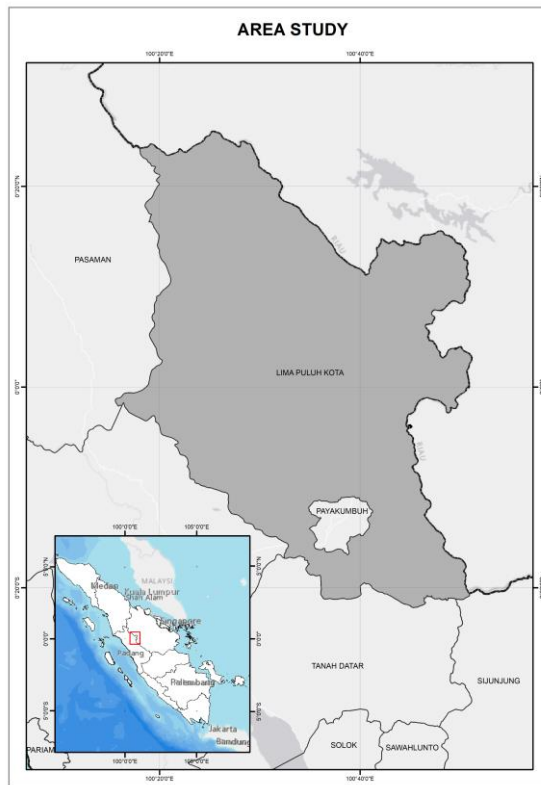


Fig. 2 Study Area

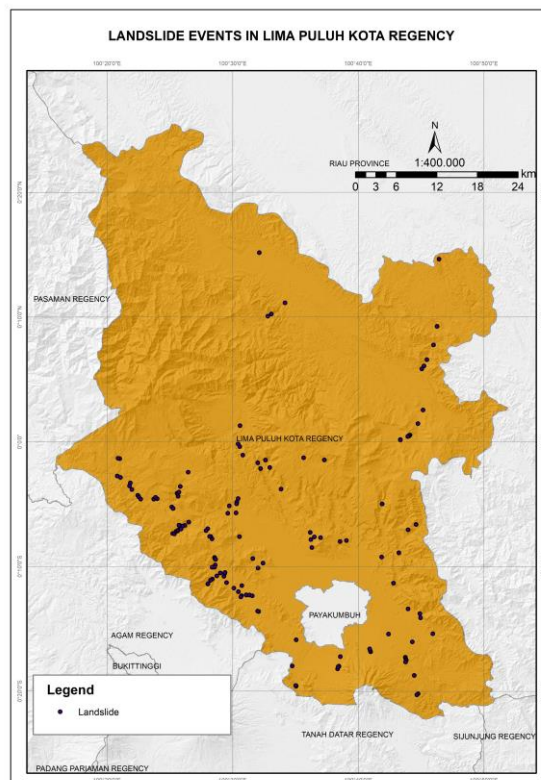


Fig. 3 Landslide Events in Lima Puluh Kota Regency

Source: Results of data analysis, 2023

### 3. RESULT AND DISCUSSION

The results of calculations based on the fuzzy logic method show the minimum and maximum values, namely 0 to 1, where the closer the value is to 0, the lower the resulting level of danger and vice versa. In the aspect factor, northeast and east are the classes with the highest number of landslides, each with 15 landslide points. In the rainfall intensity factor, 2000-2500 mm has the highest number of landslides with 77 landslide points. The curvature factor with the highest landslide occurrence is in the class -0.006 - 0.003, namely 25 landslide points. The elevation factor for the highest class of landslide occurrence is at an altitude of 581 – 728 m, namely 37 landslide points. In terms of geological factors, Miocene Sandstone is a type of rock where many landslides occur 21 points. The proximity to stream where the most landslides occur is in the 2000 – 3000 m class, namely 22 landslide points. Plantation land cover is the class with the most landslides, namely 34 points. For landforms, the Tectonic hills class is the highest, with 21 points. The highest NDVI class is 0.392 - 0.421, 21 landslide points. The slope factor that has a high incidence of landslides is in the class 18.453 - 24.180, that is, there are 37 landslide points. And for the last parameter soil, the highest incidence of landslides occurred in the Haplic Podzol class 42 points.

In the aspect factor, west and north are the classes with the lowest number of landslides with 5 landslide points each. In the rainfall intensity factor, the class that does not have landslides is the 3,500 –

4,000 mm class. The curvature factor that does not have landslide events is class -0.232 - -0.060. The elevation factors for classes that do not have landslides are at heights 1038 - 1210 m, class 1210 - 1417 m, class 1417 - 1701 m and class 1701 - 2269 m. In terms of geological factors, the classes that do not have landslides are Kuantan Formation, Rhyoandesite Volcanic, Carboniferous Carbon, Airbalam Formation, Amas Volcanic Formation, Bohorok Formation, Kota Alam Volcanic Formation, Pematang Formation, Telisa Formation, Telukkido Formation, Granite, Minor Granite Intrus, Miocene Polymictic and Mangani Porphyry. Proximity to streams that do not have landslides are in the 100 - 200 m class. Landcover factors that do not have landslides are lakes, fishponds, rivers and swamps. For the landform factor, classes that do not have landslides are Intermontane plateau, Old Volcanic Plain, Escarpment, Flow path, Volcanic foot, Upper slope, Penepplain, Karst hills, Tectonic Plate Ridge and Body of water. The NDVI factor that does not have landslides is 0.018 – 0.111. For slope factors that do not have landslides, they are class 34.997 - 40.405, class 40.405 - 46.768, class 46.768 - 55.04 and class 55.04 - 81.128. And for the last parameter soil, the classes that do not have landslides are Umbrik Andosol, Escarpment, Eutric Gleysol, Kandic Nitisol and Body of water. These results can be seen in more detail in table 1.

The results of the fuzzy sum and fuzzy product operations can be seen in the figures 4 and 5. By using  $\gamma = 0.975$ , results were obtained with an AUC value of 0.746 in model testing.

Table 1 Fuzzy Membership Calculation based on Frequency Ratio

| No | Parameter          | Class           | Pixel (Ci) | Class of pixel (Ci) (%) | Landslide Pixel (Li) | Landslide Pixel (Li) (%) | Frequency Ratio | Fuzzy Membership (FR) |
|----|--------------------|-----------------|------------|-------------------------|----------------------|--------------------------|-----------------|-----------------------|
| 1  | Aspect             | North           | 344103     | 6,57                    | 9                    | 10,11                    | 1,54            | 1,00                  |
|    |                    | Northeast       | 732151     | 13,98                   | 15                   | 16,85                    | 1,21            | 0,69                  |
|    |                    | East            | 700050     | 13,37                   | 15                   | 16,85                    | 1,26            | 0,74                  |
|    |                    | Southeast       | 647773     | 12,37                   | 11                   | 12,36                    | 1,00            | 0,49                  |
|    |                    | South           | 615405     | 11,75                   | 8                    | 8,99                     | 0,76            | 0,27                  |
|    |                    | Southwest       | 641977     | 12,26                   | 7                    | 7,87                     | 0,64            | 0,16                  |
|    |                    | West            | 617756     | 11,80                   | 5                    | 5,62                     | 0,48            | 0,00                  |
|    |                    | Northwest       | 614125     | 11,73                   | 14                   | 15,73                    | 1,34            | 0,81                  |
|    |                    | North           | 324001     | 6,19                    | 5                    | 5,62                     | 0,91            | 0,41                  |
| 2  | Rainfall Intensity | 2000 – 2500     | 2655162    | 50,71                   | 77                   | 86,52                    | 1,71            | 0,81                  |
|    |                    | 2500 – 3000     | 2395306    | 45,75                   | 6                    | 6,74                     | 0,15            | 0,07                  |
|    |                    | 3000 – 3500     | 167286     | 3,19                    | 6                    | 6,74                     | 2,11            | 1,00                  |
|    |                    | 3500 – 4000     | 18304      | 0,35                    | 0                    | 0,00                     | 0,00            | 0,00                  |
| 3  | Curvature          | -0,232 - -0,060 | 7067       | 0,13                    | 0                    | 0,00                     | 0,00            | 0,00                  |
|    |                    | -0,060 - -0,039 | 44136      | 0,84                    | 1                    | 1,12                     | 1,33            | 0,85                  |

| No | Parameter | Class                        | Pixel (Ci) | Class of pixel (Ci) (%) | Landslide Pixel (Li) | Landslide Pixel (Li) (%) | Frequency Ratio | Fuzzy Membership (FR) |
|----|-----------|------------------------------|------------|-------------------------|----------------------|--------------------------|-----------------|-----------------------|
|    |           | -0,039 - -0,025              | 159807     | 3,05                    | 1                    | 1,12                     | 0,37            | 0,24                  |
|    |           | -0,025 - -0,015              | 426780     | 8,15                    | 10                   | 11,24                    | 1,38            | 0,88                  |
|    |           | -0,015 - -0,006              | 874546     | 16,70                   | 21                   | 23,60                    | 1,41            | 0,90                  |
|    |           | -0,006 - 0,003               | 1616004    | 30,86                   | 25                   | 28,09                    | 0,91            | 0,58                  |
|    |           | 0,003 - 0,011                | 1176621    | 22,47                   | 13                   | 14,61                    | 0,65            | 0,42                  |
|    |           | 0,011 - 0,021                | 640131     | 12,22                   | 13                   | 14,61                    | 1,20            | 0,77                  |
|    |           | 0,021 - 0,039                | 254563     | 4,86                    | 4                    | 4,49                     | 0,92            | 0,59                  |
|    |           | 0,039 - 0,206                | 37686      | 0,72                    | 1                    | 1,12                     | 1,56            | 1,00                  |
| 4  | Elevasi   | 65 – 237                     | 1025804    | 19,59                   | 5                    | 5,62                     | 0,29            | 0,09                  |
|    |           | 237 – 409                    | 761290     | 14,54                   | 7                    | 7,87                     | 0,54            | 0,16                  |
|    |           | 409 – 581                    | 1003682    | 19,16                   | 14                   | 15,73                    | 0,82            | 0,24                  |
|    |           | 581 – 728                    | 649868     | 12,41                   | 37                   | 41,57                    | 3,35            | 1,00                  |
|    |           | 728 – 883                    | 613551     | 11,72                   | 24                   | 26,97                    | 2,30            | 0,69                  |
|    |           | 883 – 1038                   | 516381     | 9,86                    | 2                    | 2,25                     | 0,23            | 0,07                  |
|    |           | 1038 – 1210                  | 348748     | 6,66                    | 0                    | 0,00                     | 0,00            | 0,00                  |
|    |           | 1210 – 1417                  | 172873     | 3,30                    | 0                    | 0,00                     | 0,00            | 0,00                  |
|    |           | 1417 – 1701                  | 94259      | 1,80                    | 0                    | 0,00                     | 0,00            | 0,00                  |
|    |           | 1701 – 2269                  | 50814      | 0,97                    | 0                    | 0,00                     | 0,00            | 0,00                  |
| 5  | Geology   | Alluvium                     | 57272      | 1,09                    | 1                    | 1,12                     | 1,03            | 0,05                  |
|    |           | Andesite to Basalt           | 210834     | 4,03                    | 8                    | 8,99                     | 2,23            | 0,11                  |
|    |           | Andesite of Gunung Malintang | 257524     | 4,92                    | 6                    | 6,74                     | 1,37            | 0,07                  |
|    |           | Kuantan Formation            | 73274      | 1,40                    | 0                    | 0,00                     | 0,00            | 0,00                  |
|    |           | Rhyoandesite Volcanic        | 2032       | 0,04                    | 0                    | 0,00                     | 0,00            | 0,00                  |
|    |           | Carboniferous Carbon         | 13775      | 0,26                    | 0                    | 0,00                     | 0,00            | 0,00                  |
|    |           | Carboniferous Metamorphic    | 187797     | 3,59                    | 7                    | 7,87                     | 2,19            | 0,11                  |
|    |           | Miocene Sandstone            | 285968     | 5,46                    | 21                   | 23,60                    | 4,32            | 0,21                  |
|    |           | Airbalam Formation           | 64233      | 1,23                    | 0                    | 0,00                     | 0,00            | 0,00                  |
|    |           | Amas Volcanic Formation      | 26973      | 0,52                    | 0                    | 0,00                     | 0,00            | 0,00                  |
|    |           | Bohorok Formation            | 15257      | 0,29                    | 0                    | 0,00                     | 0,00            | 0,00                  |
|    |           | Brani Formation              | 217904     | 4,16                    | 8                    | 8,99                     | 2,16            | 0,11                  |
|    |           | Kota Alam Volcanic Formaton  | 32630      | 0,62                    | 0                    | 0,00                     | 0,00            | 0,00                  |
|    |           | Kuantan Formation            | 1848717    | 35,31                   | 20                   | 22,47                    | 0,64            | 0,03                  |
|    |           | Pematang Formation           | 58581      | 1,12                    | 0                    | 0,00                     | 0,00            | 0,00                  |
|    |           | Sangkarewang Formation       | 184117     | 3,52                    | 2                    | 2,25                     | 0,64            | 0,03                  |
|    |           | Sihapas Formation            | 833812     | 15,93                   | 1                    | 1,12                     | 0,07            | 0,00                  |
|    |           | Telisa Formation             | 462199     | 8,83                    | 0                    | 0,00                     | 0,00            | 0,00                  |
|    |           | Telukcido Formation          | 36214      | 0,69                    | 0                    | 0,00                     | 0,00            | 0,00                  |
|    |           | Totolan Formation            | 283049     | 5,41                    | 10                   | 11,24                    | 2,08            | 0,10                  |
|    |           | Granite                      | 55057      | 1,05                    | 0                    | 0,00                     | 0,00            | 0,00                  |
|    |           | Minor Granite Intrus         | 3752       | 0,07                    | 0                    | 0,00                     | 0,00            | 0,00                  |
|    |           | Miocene Polymictic           | 163        | 0,00                    | 0                    | 0,00                     | 0,00            | 0,00                  |
|    |           | Mangani Porphyry             | 9838       | 0,19                    | 0                    | 0,00                     | 0,00            | 0,00                  |
|    |           | Andesite or Dacite Porfiry   | 14514      | 0,28                    | 5                    | 5,62                     | 20,27           | 1,00                  |

| No                   | Parameter           | Class                       | Pixel (Ci) | Class of pixel (Ci) (%) | Landslide Pixel (Li) | Landslide Pixel (Li) (%) | Frequency Ratio | Fuzzy Membership (FR) |
|----------------------|---------------------|-----------------------------|------------|-------------------------|----------------------|--------------------------|-----------------|-----------------------|
| 6                    | Proximity To Stream | 0 – 100                     | 151304     | 2,89                    | 8                    | 8,99                     | 3,11            | 1,00                  |
|                      |                     | 100 – 200                   | 119709     | 2,29                    | 0                    | 0,00                     | 0,00            | 0,00                  |
|                      |                     | 200 – 300                   | 113412     | 2,17                    | 1                    | 1,12                     | 0,52            | 0,17                  |
|                      |                     | 300 – 400                   | 109305     | 2,09                    | 1                    | 1,12                     | 0,54            | 0,17                  |
|                      |                     | 400 – 500                   | 106594     | 2,04                    | 3                    | 3,37                     | 1,66            | 0,53                  |
|                      |                     | 500 – 1000                  | 511765     | 9,77                    | 13                   | 14,61                    | 1,49            | 0,48                  |
|                      |                     | 1000 – 2000                 | 908070     | 17,34                   | 19                   | 21,35                    | 1,23            | 0,40                  |
|                      |                     | 2000 – 3000                 | 757523     | 14,46                   | 22                   | 24,72                    | 1,71            | 0,55                  |
|                      |                     | 3000 – 4000                 | 629997     | 12,03                   | 4                    | 4,49                     | 0,37            | 0,12                  |
|                      |                     | >5000                       | 1829499    | 34,93                   | 18                   | 20,22                    | 0,58            | 0,19                  |
| 7                    | Landcover           | Lake                        | 13781      | 0,26                    | 0                    | 0,00                     | 0,00            | 0,00                  |
|                      |                     | Fishpond                    | 157        | 0,00                    | 0                    | 0,00                     | 0,00            | 0,00                  |
|                      |                     | Forest                      | 1853101    | 35,40                   | 6                    | 6,74                     | 0,19            | 0,09                  |
|                      |                     | Shrubs                      | 377507     | 7,21                    | 8                    | 8,99                     | 1,25            | 0,57                  |
|                      |                     | Moor                        | 972372     | 18,57                   | 24                   | 26,97                    | 1,45            | 0,66                  |
|                      |                     | River                       | 19627      | 0,37                    | 0                    | 0,00                     | 0,00            | 0,00                  |
|                      |                     | Settlement                  | 73971      | 1,41                    | 2                    | 2,25                     | 1,59            | 0,72                  |
|                      |                     | Paddyfield                  | 400244     | 7,64                    | 15                   | 16,85                    | 2,20            | 1,00                  |
|                      |                     | Plantation                  | 1522509    | 29,08                   | 34                   | 38,20                    | 1,31            | 0,60                  |
|                      |                     | Swamp                       | 2192       | 0,04                    | 0                    | 0,00                     | 0,00            | 0,00                  |
| 8                    | Landform            | Alluvial plain              | 189062     | 3,61                    | 1                    | 1,12                     | 0,31            | 0,03                  |
|                      |                     | Intermontane plateau        | 28169      | 0,54                    | 0                    | 0,00                     | 0,00            | 0,00                  |
|                      |                     | Kolovial plain              | 23372      | 0,45                    | 2                    | 2,25                     | 5,03            | 0,48                  |
|                      |                     | Tectonic plain              | 443270     | 8,47                    | 3                    | 3,37                     | 0,40            | 0,04                  |
|                      |                     | Volcanic plain              | 179450     | 3,43                    | 11                   | 12,36                    | 3,61            | 0,34                  |
|                      |                     | Old Volcanic Plain          | 65252      | 1,25                    | 0                    | 0,00                     | 0,00            | 0,00                  |
|                      |                     | Escarpment                  | 8139       | 0,16                    | 0                    | 0,00                     | 0,00            | 0,00                  |
|                      |                     | Tectonic Escarpment Plateau | 67950      | 1,30                    | 1                    | 1,12                     | 0,87            | 0,08                  |
|                      |                     | Volcanic intrusion          | 16814      | 0,32                    | 3                    | 3,37                     | 10,50           | 1,00                  |
|                      |                     | Flow path                   | 1526       | 0,03                    | 0                    | 0,00                     | 0,00            | 0,00                  |
|                      |                     | Volcanic foot               | 30222      | 0,58                    | 0                    | 0,00                     | 0,00            | 0,00                  |
|                      |                     | Upper slope                 | 58020      | 1,11                    | 0                    | 0,00                     | 0,00            | 0,00                  |
|                      |                     | Lower slope                 | 97873      | 1,87                    | 6                    | 6,74                     | 3,61            | 0,34                  |
|                      |                     | Middle slope                | 77625      | 1,48                    | 2                    | 2,25                     | 1,52            | 0,14                  |
|                      |                     | Tectonic mountains          | 2134005    | 40,76                   | 16                   | 17,98                    | 0,44            | 0,04                  |
|                      |                     | Old Volcanic Mountains      | 465136     | 8,88                    | 14                   | 15,73                    | 1,77            | 0,17                  |
|                      |                     | Penepplain                  | 28327      | 0,54                    | 0                    | 0,00                     | 0,00            | 0,00                  |
|                      |                     | Karst hills                 | 46365      | 0,89                    | 0                    | 0,00                     | 0,00            | 0,00                  |
|                      |                     | Tectonic hills              | 1083309    | 20,69                   | 21                   | 23,60                    | 1,14            | 0,11                  |
|                      |                     | Old Volcanic Hills          | 88538      | 1,69                    | 9                    | 10,11                    | 5,98            | 0,57                  |
| Tectonic Plate Ridge | 92892               | 1,77                        | 0          | 0,00                    | 0,00                 | 0,00                     |                 |                       |
| Body of water        | 10153               | 0,19                        | 0          | 0,00                    | 0,00                 | 0,00                     |                 |                       |
| 9                    | NDVI                | 0,018 - 0,111               | 58704      | 1,12                    | 0                    | 0,00                     | 0,00            | 0,00                  |

| No | Parameter | Class             | Pixel (Ci) | Class of pixel (Ci) (%) | Landslide Pixel (Li) | Landslide Pixel (Li) (%) | Frequency Ratio | Fuzzy Membership (FR) |
|----|-----------|-------------------|------------|-------------------------|----------------------|--------------------------|-----------------|-----------------------|
|    |           | 0,111 - 0,183     | 77777      | 1,48                    | 2                    | 2,25                     | 1,51            | 0,78                  |
|    |           | 0,183 - 0,235     | 157980     | 3,02                    | 5                    | 5,62                     | 1,86            | 0,96                  |
|    |           | 0,235 - 0,278     | 272953     | 5,21                    | 9                    | 10,11                    | 1,94            | 1,00                  |
|    |           | 0,278 - 0,314     | 479636     | 9,16                    | 13                   | 14,61                    | 1,60            | 0,82                  |
|    |           | 0,314 - 0,342     | 697317     | 13,31                   | 13                   | 14,61                    | 1,10            | 0,57                  |
|    |           | 0,342 - 0,368     | 986361     | 18,83                   | 14                   | 15,73                    | 0,84            | 0,43                  |
|    |           | 0,368 - 0,392     | 1098358    | 20,97                   | 6                    | 6,74                     | 0,32            | 0,17                  |
|    |           | 0,392 - 0,421     | 987348     | 18,85                   | 21                   | 23,60                    | 1,25            | 0,65                  |
|    |           | 0,421 - 0,628     | 421847     | 8,05                    | 6                    | 6,74                     | 0,84            | 0,43                  |
| 10 | Slope     | 0 - 6,363         | 1025804    | 19,59                   | 5                    | 5,62                     | 0,29            | 0,09                  |
|    |           | 6,363 - 12,408    | 761290     | 14,54                   | 7                    | 7,87                     | 0,54            | 0,16                  |
|    |           | 12,408 - 18,453   | 1003682    | 19,16                   | 14                   | 15,73                    | 0,82            | 0,24                  |
|    |           | 18,453 - 24,180   | 649868     | 12,41                   | 37                   | 41,57                    | 3,35            | 1,00                  |
|    |           | 24,180 - 29,588   | 613551     | 11,72                   | 24                   | 26,97                    | 2,30            | 0,69                  |
|    |           | 29,588 - 34,997   | 516381     | 9,86                    | 2                    | 2,25                     | 0,23            | 0,07                  |
|    |           | 34,997 - 40,405   | 348748     | 6,66                    | 0                    | 0,00                     | 0,00            | 0,00                  |
|    |           | 40,405 - 46,768   | 172873     | 3,30                    | 0                    | 0,00                     | 0,00            | 0,00                  |
|    |           | 46,768 - 55,04    | 94259      | 1,80                    | 0                    | 0,00                     | 0,00            | 0,00                  |
|    |           | 55,04 - 81,128    | 50814      | 0,97                    | 0                    | 0,00                     | 0,00            | 0,00                  |
| 11 | Soil      | Umbric Andosol    | 34098      | 0,65                    | 0                    | 0,00                     | 0,00            | 0,00                  |
|    |           | Eскарment         | 8132       | 0,16                    | 0                    | 0,00                     | 0,00            | 0,00                  |
|    |           | District Gleysol  | 257040     | 4,91                    | 4                    | 4,49                     | 0,92            | 0,33                  |
|    |           | Eutric Gleysol    | 44398      | 0,85                    | 0                    | 0,00                     | 0,00            | 0,00                  |
|    |           | District Cambisol | 292858     | 5,59                    | 2                    | 2,25                     | 0,40            | 0,15                  |
|    |           | Lithic Cambisol   | 59060      | 1,13                    | 2                    | 2,25                     | 1,99            | 0,72                  |
|    |           | Oxic Cambisol     | 234474     | 4,48                    | 7                    | 7,87                     | 1,76            | 0,64                  |
|    |           | Gleyic Luvisol    | 128073     | 2,45                    | 6                    | 6,74                     | 2,76            | 1,00                  |
|    |           | Oxic Latosol      | 101574     | 1,94                    | 2                    | 2,25                     | 1,16            | 0,42                  |
|    |           | Kandic Nitisol    | 15064      | 0,29                    | 0                    | 0,00                     | 0,00            | 0,00                  |
|    |           | Haplic Podzol     | 2119343    | 40,48                   | 42                   | 47,19                    | 1,17            | 0,42                  |
|    |           | Kandic Podzol     | 1863237    | 35,59                   | 23                   | 25,84                    | 0,73            | 0,26                  |
|    |           | ROC               | 67944      | 1,30                    | 1                    | 1,12                     | 0,87            | 0,31                  |
|    |           | Body of water     | 10167      | 0,19                    | 0                    | 0,00                     | 0,00            | 0,00                  |

Source : Data Processing, 2023

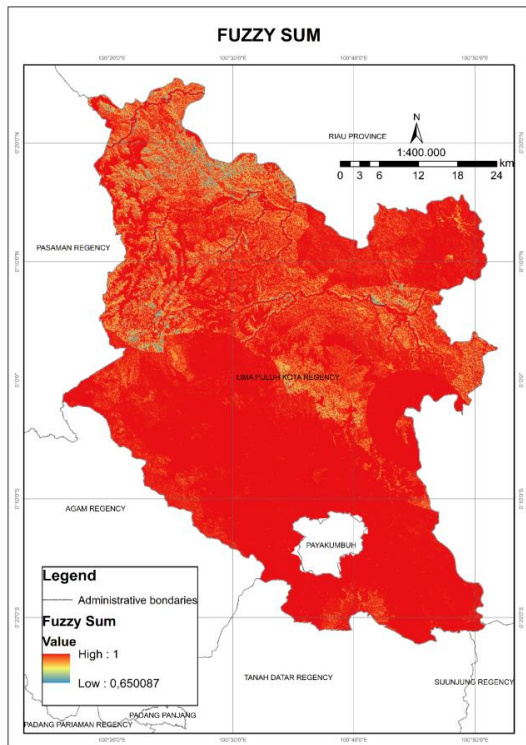


Fig. 4 Fuzzy Sum

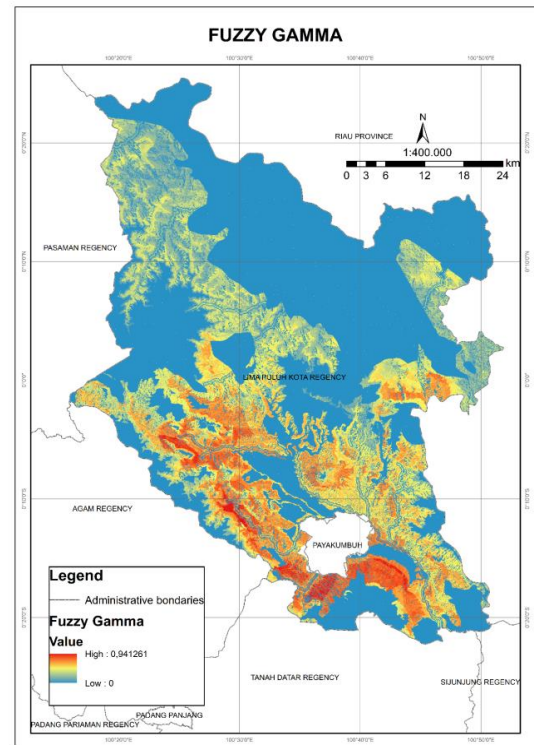


Fig. 6 Fuzzy Gamma

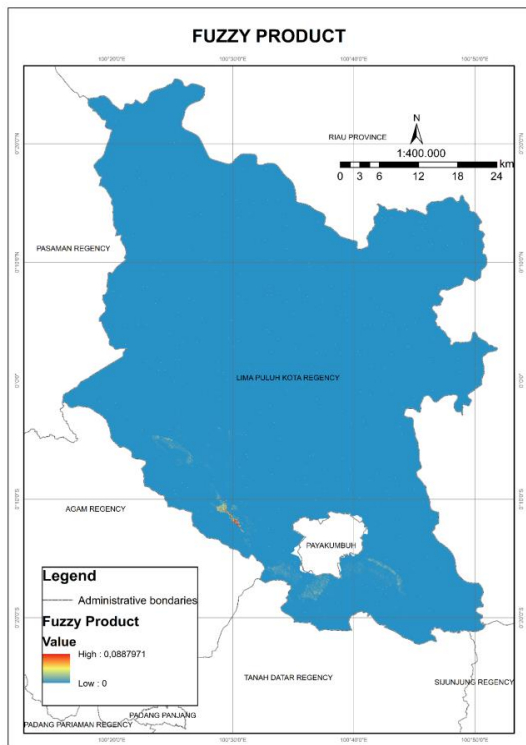


Fig. 5 Fuzzy Product

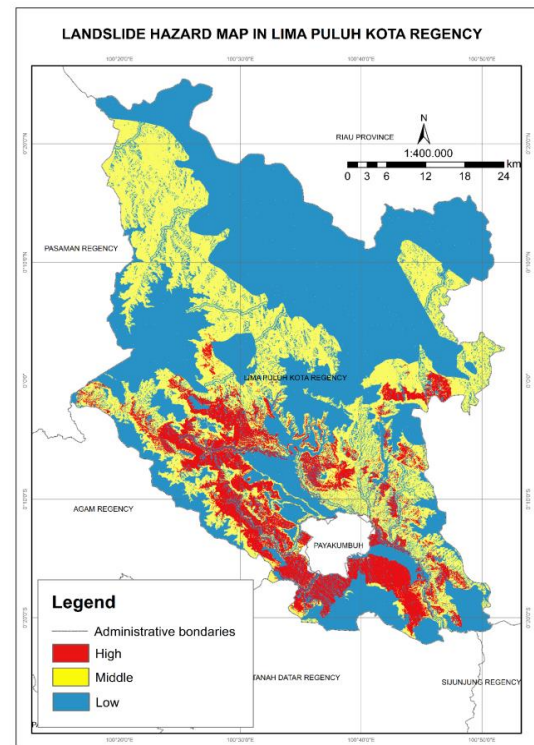


Fig. 7 Landslide Hazard Map Lima Puluh Kota Regency



Table 2 Landslide Hazard Results using the Fuzzy Gamma Operator

| No | Class  | Area (ha) | Percent (%) |
|----|--------|-----------|-------------|
| 1  | High   | 28.463    | 8,79        |
| 2  | Middle | 76.544    | 23,64       |
| 3  | Low    | 218.820   | 67,57       |

Source: data processing, 2023

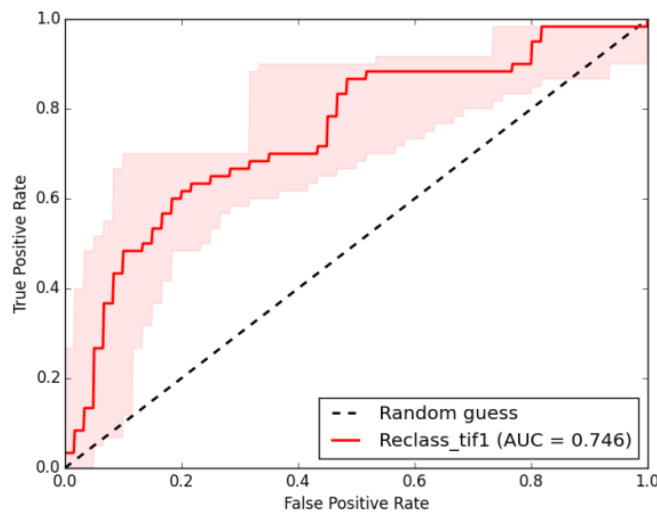


Fig. 8 ROC anad AUC

#### 4. CONCLUSION

The landslide hazard map based on the Fuzzy Gamma operator based on the Frequency Ratio membership function has varying levels of danger. The susceptibility map results show that the most suitable one with  $\gamma = 0.975$  is an AUC value of 0.746, which means the level of accuracy of the resulting map is high. The model produces high landslide susceptibility classes covering an area of 28,463 ha (8.79%), medium landslide susceptibility covering an area of 76,544 ha (23.64%) and low landslide susceptibility covering an area of 218,820 ha (67.57%). Thus, awareness of the danger of landslides needs to be paid attention to in the western and central regions of Limapuluh Kota Regency because that is where the concentration of landslide vulnerability is high and medium

#### 5. ACKNOWLEDGEMENTS

This research can be carried out smoothly, because of the assistance and cooperation from various parties. Therefore, the author would like to thank the Rector of Universitas Negeri Padang.

#### 6. REFERENCES

[1] Ahyuni, Susetyo, B.B, Oktari, F., Nur, H., Aziz, A. (2021). The Difference of Landslide-Prone Areas Between Heuristic and Statistical

Methods in Lima Puluh Kota regency. Sumatra Journal of Disaster, Geography and Geography Education Vol.5 No2, Pp. 107-114., 5, 107–114.

[2] Bui, D. T., Pradhan, B., Lofman, O., Revhaug, I., & Dick, O. B. (2012). Spatial prediction of landslide hazards in Hoa Binh province (Vietnam). *Catena. A Comparative Assessment of the Efficacy of Evidential Belief Functions and Fuzzy Logic Models*, 96, 28–40.

[3] Ilanloo, M. (2011). A Comparative Study of Fuzzy Logic Approach for Landslide Susceptibility mapping using GIS: An experience of Karaj Dam Basin in Iran. *Procedia Social and Behavioral Sciences*, 19, 668–676. [www.sciencedirect.com](http://www.sciencedirect.com)

[4] Kanungo, D. P., Arora, M. K., Sarkar, S., & Gupta, R. P. (2006). A comparative study of conventional, ANN black box, fuzzy and combined neural and fuzzy weighting procedures for landslide susceptibility zonation in Darjeeling Himalayas. *Engineering Geology*, 85, 347–366.

[5] Liu, J. G., Mason, P. J., Clerici, N., Chen, S., Davis, A., Miao, F., Deng, F. L., & Liang, L. (2004). Landslide hazard assessment in the Three Gorges area of the Yangtze River using ASTER imagery. *Geomorphology*, 61, 171–187.

- [6] Mandal, S., Mondal, S. (2019). *Statistical Approaches for Landslide Susceptibility Assesment and Prediction*. Springer International Publishing AG.
- [7] Mijani, N., Samani, N. N. (2017). Comparison of Fuzzy-Based Models in Landslide Hazard Mapping. *The International Archives of the Photogrammetry, Remote Sensing and Spatial and Spatial Information Sciences*, Vol XLII-4. <https://isprs-archives.copernicus.org/articles/XLII-4-W4/407/2017/>
- [8] Mitchell, T. M. (1997). *Machine learning* (p. 414). McGraw-Hill.
- [9] Pourghasemi, H. R., Pradhan, B., & Gokceoglu, C. (2012). Application of fuzzy logic and analytical hierarchy process (AHP) to landslide susceptibility mapping at Haraz watershed, Iran. *Natural Hazards*, 63, 965–996.
- [10] Pradhan, B., & Lee, S. (2009). Delineation of landslide hazard areas using frequency ratio, logistic regression and artificial neural network model at Penang Island, Malaysia. *Environmental Earth Sciences*, 60, 1037–1054.
- [11] Pradhan, B. (2010). Remote sensing and GIS-based landslide hazard analysis and cross validation using multivariate logistic regression model on three test areas in Malaysia. *Advances in Space Research*, 45, 1244–1256.
- [12] Sezer, E. A., Pradhan, B., & Gokceoglu, C. (2011). Manifestation of an adaptive neuro-fuzzy model on landslide susceptibility mapping 38(7),. Klang Valley, Malaysia. *Expert Systems with Applications*, 38(7), 8208–8219.
- [13] Tangestani, M. . (2009). A Comparative Study of Dempster-Shafer and Fuzzy Models for Landslide Susceptibility Mapping Using A GIS : An Experience from Zagros Mountains, SW Iran. *Journal of Asian Earth Sciences*. [www.elsevier.com/locate/jaes](http://www.elsevier.com/locate/jaes)
- [14] Van Westen, C. J., Rengers, N., & Soeters, R. (2003). Use of geomorphological information in indirect landslide susceptibility assessment. *Natural Hazards*. 30, 399–419.
- [15] Xie, Z., Chen, G., Meng, X., Zhang, Y., Qiao, L., Tan, L. (2017). A Comparative Study of Landslide Susceptibility Mapping Using Weight of Evidence, Logistic Regression and Support Vector Macjine and Evaluated by SBAS-InSAR Monitoring. *Zhouqu to Wudu Segment in Bailong River Basin, China*, 76, 313. <https://link.springer.com/article/10.1007/s12665-017-6640-7>
- [16] Zhu, A. X., Wang, R. X., Qiao, J., Chen, Y., Cai, Q., & Zhou, C. (2004). Mapping landslide susceptibility in the Three Gorges area, China using GIS, expert knowledge and fuzzy logic (pp. 385–391). In: Y. Chen (Ed.), *GIS and remote sensing in hydrology*. Water Resources and Environment, IAHS Publication 289 (IAHS Red Book), International Association of Hydrological Sciences, Wallingford, UK, 385–391.